IEEE Access
Multidisciplinary | Rapid Review | Open Access Journal

Received 4 December 2022, accepted 14 December 2022, date of publication 16 December 2022, date of current version 31 January 2023.

Digital Object Identifier 10.1109/ACCESS.2022.3230062

METHODS

# Multi-Task Hybrid Scheduling Scheme in FC-AE-1553 Multi-Level Switching Networks

**HAO LI[1], NINGNING LU[2], HAO WANG[3], LIHUA WU[3], JING WU[1], (Member, IEEE), HAO JIANG[1], (Member, IEEE), AND JIANGUO ZHOU[1]**

[1]School of Electronic Information, Wuhan University, Wuhan 430072, China
[2]54th Research Institute, China Electronics Technology Group Corporation, Beijing 100043, China
[3]Wuhan Second Ship Design and Research Institute, Wuhan 430205, China

Corresponding author: Jing Wu (wujing@whu.edu.cn)

**ABSTRACT** Given the increasing need of avionics communications and ship electromechanical communications for reliability and real-time transmission, current scheduling schemes waste bandwidth resources. They increase delay because of the low concurrency and the inefficiency of data transmissions in FC-AE-1553 multi-level switching networks. In this study, we first analyze the characteristics of different tasks in the field of avionics communication and establish the FC-AE-1553 network model. We then propose a multi-task hybrid scheduling scheme that includes a static scheduling scheme based on the flow and common divisors of the periods to improve the utilization of bandwidth while ensuring the periodic transmission of deterministic tasks. Further, we exhibit a dynamic bandwidth allocation scheme based on flow and credit ranking to increase throughput and fairness while decreasing the delay of burst tasks. Specifically, to ensure the periodic transmission of deterministic tasks, we divide the transmission time slots according to the common divisor of the period and schedule them in ascending order of period and flow. We update the weights of the credit ranking and flow online, and schedule them in descending order of weight size. The experimental results show that our schemes improve the bandwidth utilization of deterministic tasks by 10% and can balance the throughput and delay of the network. By improving the bandwidth utilization of deterministic tasks, we can provide a better quality of service for burst tasks. When the network can balance its throughput and delay, this shows that the network is efficient and stable.

**INDEX TERMS** Avionics communication, bandwidth, common divisor, DBA, FC-AE-1553, schedule, ship electromechanical communication.

## I. INTRODUCTION

FC-AE-1553 [1], [2] has the advantages of a fast transmission rate, low bit error rate, good concurrency, and compatibility with the MIL-STD-1553B protocol [3], [4]. It is widely used in avionics communication in-module systems [5], [6] and ship electromechanical communication in-cabin systems [7]. Because of the increasing number and types of terminals, diversification of tasks, and more frequent data transmission with inter-cabin networks, single-level switching networks are far from sufficient to meet demands [8], [9]. In addition, the scheduling scheme plays a vital role in the deployment and application of the FC-AE-1553 network. Therefore, this study aims to investigate the scheduling scheme of the FC-AE-1553 multi-level switching network.

Generally, there are three scheduling mechanisms for the FC-AE-1553 multi-level switching network: the distributed-based scheduling mechanism [10], cache-based scheduling mechanism [11], and centralized-based scheduling mechanism [12]. The distributed-based scheduling mechanism uses peer-to-peer communication [13]. There is a network controller (NC) in every switching domain, the data transmission within the switching domain is controlled by the NC of this switching domain, and the data transmission

The associate editor coordinating the review of this manuscript and approving it for publication was Tianhua Xu.

between different switching domains is negotiated by all the NCs. However, it lacks end-to-end control and data transmission management, and an increase in interactive signaling reduces bandwidth utilization [14]. The cache-based scheduling mechanism uses step-by-step communication [15] with a NC for each switching domain and a master network controller (MNC) for the entire network. When data transmission crosses different switching domains, it must be scheduled in three steps. First, after the source network terminals (NTs) send a bandwidth request to the NC, each NC determines the sending time slot of data from the source NT in the respective domain to the cross-domain switches. Next, the NCs request bandwidth resources from the MNC during a specialized period in a cycle. After collecting all requests, the MNC calculates the bandwidth allocation scheme between the cross-domain switches. Finally, data transmission from the cross-domain switch to the destination NT is controlled by the NC in the destination NT switching domain. The cache-based scheduling mechanism is the most complex and increases the delay in this manner. The centralized scheduling mechanism has only one MNC to control the data transmission in the same switching domain and different switching domains. Although the most complicated scheduling calculation increases the computational load of the MNC, it can be solved using high-performance computers. In addition, to meet the requirements of high reliability and high data transmission rate in cabins, the centralized scheduling mechanism can guarantee the consistency of data transmission and ensure unified resource allocation for the whole network [16].

The application tasks in the FC-AE-1553 network include deterministic tasks (DTs) for monitoring equipment, burst tasks (BTs) between personnel or general equipment, and immediacy tasks (ITs) for control equipment [17], [18]. A DT is periodic. In [19], it was found to be easy to derive the optimal scheduling strategy according to the constant number and length of DTs. However, with the proliferation of applications in avionics communication in-module systems and ship electromechanical communication in-cabin systems, the number and length of DTs will change, and a flexible scheduling mechanism to accommodate the variations in DTs is urgently needed. The generation time, source and destination addresses, and length of a BT are all random. The current main scheduling schemes for BTs include the dynamic bandwidth allocation scheme based on flow (DBA-F) [15], dynamic bandwidth allocation scheme based on credit ranking (DBA-C) [19], [20], fixed-length slot scheduling algorithm [19], and proportional allocation scheduling algorithm [21]. DBA-F and DBA-C are typical examples of such schemes. DBA-F can guarantee throughput and improve bandwidth utilization. However, the bandwidth requirements for low-speed tasks may be consistently unfulfilled, which leads to task starvation. The credit ranking refers to the difference between the end-to-end requested bandwidth resources and the actual allocated bandwidth resources. Each NT updates its credit ranking according to the data sent in the current period. If its credit ranking is higher, its next request is more likely to be satisfied. This can reduce delays and improve fairness, but the throughput cannot be guaranteed. An IT has the highest priority and should be sent immediately after it has been generated by the NC. The preemptive scheduling scheme ensures the timeliness of ITs by interrupting the transmission of DTs and BTs.

With the increase of terminals in the FC-AE-1553 network, and due to the different requirements of communication tasks on the delay and delay jitter, the development of a multi-task scheduling scheme in FC-AE-1553 multi-level switching networks faces many challenges. First, because the FC-AE-1553 network is a multi-level structure, it is difficult to make a quick and consistent decision for end-to-end transmissions while maintaining flexibility. Second, with the rapid development of networks, the types of tasks are becoming increasingly numerous, and adapting to the dynamically changing characteristics of multiple types of tasks is a new challenge.

In this paper, we propose a multi-task hybrid scheduling scheme (MTHSS) for an FC-AE-1553 multi-level switching network. We continue to use the fixed-length slot scheduling, and the cycle is divided into many fixed-length time slots. First, to adapt to the changes in tasks, specialized time slots are set to collect BT and DT bandwidth requests and calculate the bandwidth allocation results. We then divide the remaining time slots into DT transmission time slots and BT transmission time slots. In their own transmission slots, according to their characteristics, the corresponding scheduling algorithm is used to improve the transmission efficiency as much as possible. Finally, owing to the small number of ITs, we reserved the IT transmission time in each time slot to ensure timeliness. Dividing a cycle into three parts and scheduling according to the respective characteristics of tasks can adapt to the dynamic changes in the tasks and improve scheduling flexibility and scheduling efficiency. The main contributions of this study are as follows.

- The MTHSS for multi-level switching networks with the highest global control is proposed. First, we adopt the centralized scheduling mechanism, which controls the transmission of all data, making quick and consistent decisions for end-to-end transmissions. Second, we partition the time slots according to the number and length of the tasks. In particular, we first determine the DT scheduling area according to the number and length of the DTs, and the remaining time slots are the BT scheduling areas. This can improve the overall transmission utilization and scheduling flexibility. Finally, scheduling with an appropriate scheme according to the characteristics of tasks can adapt to the dynamic changes in multiple tasks.
- A static scheduling scheme based on the flow and common divisors of the periods (SS-FP) is proposed for DTs. First, we treat a cluster cycle as the scheduling unit, where the cluster cycle is the least common multiple of all the DT cycles. At the beginning of each cluster cycle, the MNC perceives whether the DTs change dynamically. If they do, the MNC recalculates the bandwidth

allocation scheme. Then, we convert the scheduling problem of the cluster cycle into the packing problem, divide time slots into aggregated areas according to the cycles of DTs, and schedule DTs with the same cycle in the same aggregated time slots to ensure the periodic transmission of the DTs. Finally, according to the order of the common factor of the DT cycle from small to large, the aggregate time slots with a small common factor are filled first to ensure periodic transmission while improving the time slot utilization of the DTs.

- A dynamic bandwidth allocation scheme based on flow and credit ranking (DBA-FC) is proposed for BTs. First, considering both the bandwidth request of the current BTs and the bandwidth allocation result of the last scheduling can combine the advantages of both DBA-F and DBA-C to balance the fairness and efficiency of bandwidth utilization. Second, because a BT is random, if the model parameters are not updated online, this will lead to an unstable effect on dynamic bandwidth allocation. The results of comparative experiments demonstrate that the online updating of the model parameters can adapt to the dynamic characteristics of BTs.

The remainder of this paper is organized as follows. Section II describes the research related to the task scheduling of the FC-AE-1553 network. Then the FC-AE-1553 network model and specific implementation process of the scheduling scheme are presented in Section III. Section IV presents an analysis of the related performance evaluation results. Finally, a summary and an outlook for future work are presented in Section V.

## II. RELATED WORK

The FC-AE-1553 network supports point-to-point, arbitrated loop, and switching topologies, where point-to-point and arbitration ring topologies are suitable for networks with a small number of NTs. However, in avionics communication in-module systems and ship electromechanical communication in-cabin systems, there are many NTs in each cabin and a large amount of data between cabins. Therefore, a switching network topology is more suitable for the in-cabin system. Qian et al. [16] proposed a distribution-based scheduling mechanism for an FC-AE-1553 multi-level switching network. Data transmission within the same switching domain is responsible for the NC of the respective switching domain, which reduces the computational requirements of the NCs and does not affect the data transmission in the respective switching domains. However, the data transmission between different switching domains needs to be negotiated together by all NCs, which increases interactive signaling and thus reduces bandwidth utilization. Wang et al. [15] proposed a cache-based scheduling mechanism for an FC-AE-1553 multi-level switching network. As with the distribution-based scheduling mechanism, the NC of each switching domain is responsible for data transmission within its respective switching domain. To decrease interactive signaling, data transmission between different switching domains is controlled by the MNC. However, it is necessary to increase the cache of the switches and the delay in data transmission across different switching domains. In addition, these two methods cannot make quick and consistent decisions regarding end-to-end transmissions; therefore, it is difficult to ensure the consistency of data transmission. He et al. [19] proposed a centralized scheduling mechanism for the FC-AE-1553 multi-level switching network that can guarantee the consistency of aerospace data transmission. The MNC obtains global information of network resources and performs global provisioning and optimization of resources according to requirements, which improves the efficiency of the overall utilization of network resources.

Because different communication tasks have different requirements for bandwidth and delay, a reasonable multitask scheduling mechanism needs to be designed to meet the transmission requirements of each task. Li [22] and He [19] used a static scheduling scheme with fixed time slots reserved for DT scheduling. Theoretically, static scheduling can calculate the best scheduling scheme for DTs; however, when the number and length of DTs change, the transmission of DTs may conflict when using a static scheduling scheme. Zhan [23] and Wu [20] used the DBA-C for BTs. The source and destination ports of the task with a higher credit ranking are preferentially allocated bandwidth, and the credit ranking is recalculated according to whether the demand is satisfied. This method ensures the fairness of the network and reduces the transmission delay; however, it decreases bandwidth utilization. Wang [15] proposed a first-time optimal adaptation scheduling scheme based on the flow that converts the multipoint-to-multipoint transmission problem into a one-dimensional packing problem. This reduces the delay for high-speed tasks; however, low-speed tasks may suffer from starvation. Because ITs have the highest requirements for delay and reliability, a preemptive scheduling scheme is the most effective. To prevent bandwidth preemption of ITs from affecting the transmission of other tasks, He [19] reserved the protection time at the end of each time slot, which can ensure that data transmission will not be disrupted by the insertion of ITs.

To address the challenges of scheduling in FC-AE-1553 networks, we propose the MTHSS for a FC-AE-1553 multi-level switching network based on a summary of the above related work. In our scheme, we adopt a centralized scheduling mechanism. This mechanism has higher global control and can flexibly use the dynamic bandwidth allocation algorithm with high reliability. When the NC of a switching domain in the distributed or cached FC-AE-1553 multi-level switching network breaks down, it is necessary to turn the network into a centralized scheduling mechanism to ensure normal operation. Lan et al. [24] proposed an autonomous interdevice bus control-transfer protocol. If the failure of the MNC leads to network paralysis, the highest priority NT will autonomously acquire bus control, and the communication will be self-healing, which prevents the network from failing due to the ineffectiveness of MNC. Therefore, when using the centralized scheduling solution with a self-healing mechanism, we do not need to worry about the network going down owing to the paralysis of the MNC. For DTs, we designed the SS-FP, which ensures the periodic execution of data transmission and adapts to changes in DTs. For BTs, we propose DBA-FC, which can adapt to random changes in the ratio of high-speed and low-speed tasks and ensure the stability of throughput and delay. We reserved the sending time for ITs to protect the network from failure due to a delay or loss of an IT.

## III. DESIGN OF THE MTHSS

This section presents a formal system model of the FC-AE-1553 network. We also illustrate the principles of SS-FP and DBA-FC separately. Finally, the combined application of the two schemes is explained.

### A. FC-AE-1553 SYSTEM MODEL

A model of the FC-AE-1553 network is shown in Fig. 1. The network architecture is divided into three parts (from top to bottom): the network control layer, network switching layer, and network business layer. The network control layer is responsible for transmission-request queries, time synchronization, and data transmission coordination. NC is different from the controller of the software defined network (SDN). First, the NC generates tasks. Next, it sends scheduling schemes instead of flow tables, that is, the network switching layer only forwards the data, and does not modify or discard it. Finally, because the NC sends the scheduling schemes, which contain the specific sending time slot and the occupied link bandwidth resources of each task, not just the rules for data stream forwarding, the control of the NC is more specific and defined. Communication transmission between all terminals is achieved by placing many private switches in the network-switching layer. In the network business layer, when two NTs are connected to the same switch, it means that both NTs are in the same switching domain. When the data transmission of two NTs needs to cross several switches, this implies that both NTs are in different switching domains.

The tasks in avionics communication in-module systems and ship electromechanical communication in-cabin systems can be summarized into three types: DTs, BTs, and ITs. DTs are periodic tasks that are the most sensitive to delay jitter. BTs are generated between various nodes and occupy approximately 96% of the bandwidth. ITs are control instructions with strong time sensitive requirements that can only be generated by the NC and sent to the NTs. The NTs must execute the corresponding operations within a set time threshold. The specific characteristics of the three tasks are listed in Table 1.

The task attribute in the FC-AE-1553 network are expressed as

$$Task_i = \{id, source, destination, period, length\}. \quad (1)$$

The subscript $i$ denotes the number of tasks, $id$ denotes the identifier of the task, $source$ denotes the address of the

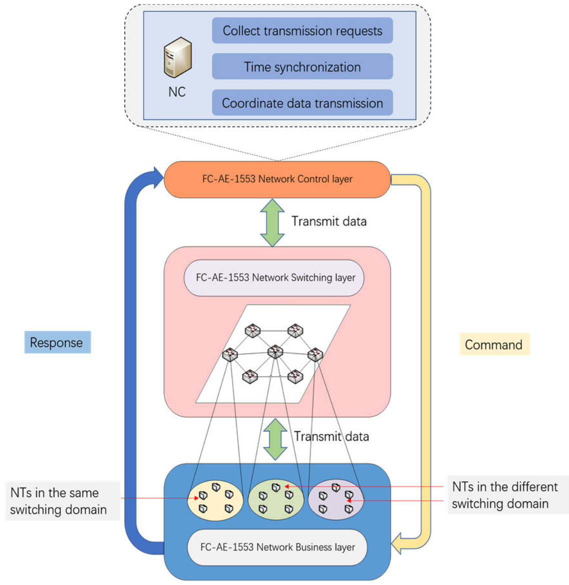


**FIGURE 1.** FC-AE-1553 network model.

**TABLE 1.** Characteristics of the three task types [15].

| Task type | Direction of data transmission | Maximum allowable delay | Data length | Bandwidth |
|---|---|---|---|---|
| DT | NC→NT<br>NT→NC | 500 μs to 8 ms | 512 Bytes | 4% |
| BT | NC→NT<br>NT→NT<br>NT→NC | 100 ms | 64 KBytes | 96% |
| IT | NC→NT | 50μs | 100 Bytes | Less than 0.1% |

source node, $destination$ denotes the address of the destination node, $period$ denotes the period of the DTs, and BTs are not periodic. Here, $length$ denotes the amount of requested bandwidth.

We define the task set $T$, where the NC collects bandwidth requests for every scheduling cycle and updates the set $T$ as follows:

$$T = \{Task_1, Task_2, \cdots, Task_n\}. \quad (2)$$

We divide the bandwidth resources of each link into $K$ time slots. The link bandwidth time slot matrix $B$ is

$$B = [b_{ij}]_{2N*K} = \begin{bmatrix} b_{11} & \cdots & b_{1K} \\ \vdots & & \vdots \\ b_{N1} & \cdots & b_{NK} \\ b_{(N+1)1} & \cdots & b_{(N+1)K} \\ \vdots & & \vdots \\ b_{(2N)1} & \cdots & b_{(2N)K} \end{bmatrix}. \quad (3)$$

The fundamental period (FP) is divided into $K$ time slots. The element $b_{ij}$ represents the j-th time slot of the i-th link and $b_{ij} = \{0, 1\}$. When $b_{ij} = 0$, the j-th time slot of the

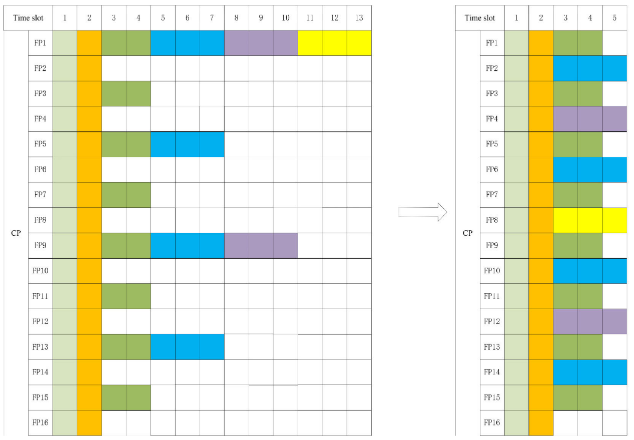


**FIGURE 2.** Folded diagram of DT time slot allocation.

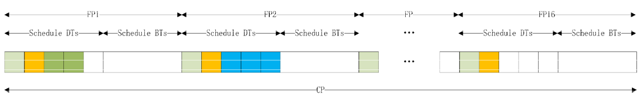


**FIGURE 3.** Unfolded diagram of DT time slot allocation.

sending/receiving link numbered $i$ is not occupied, and vice versa. The links are all full-duplex links. When $i \leq N$, $b_{ij}$ is the time slot of the sending link; when $i > N$, $b_{ij}$ denotes the time slot of the receiving link.

### *B. SS-FP*

Because DTs only exist between the NC and NT, when the sending and receiving time slots of the NC do not conflict, the normal transmission of the DTs can be guaranteed. Therefore, we must determine the scheduling cycle of the DTs. We calculate the least common multiple (LCM) and the greatest common divisor (GCD) of all periods of DTs and define the cluster period (CP) to be the LCM and the FP to be the GCD so that each DT can be guaranteed to be scheduled at most once in an FP and at least once in a CP. After a CP, if the number and length of tasks do not change, the scheduling result of the next CP will be the same as that of the last one. Therefore, we define the CP as the scheduling period of a DT, whereas the scheduling of a BT is in terms of the FP. The relationship between the CP and FP is

$$s = \frac{CP}{FP}, \quad s \in Z \tag{4}$$

Fig. 2 shows a diagram of the time slot allocation of the NC sending link in a CP. There are six DTs from the NC to the NTs, and a CP consists of 16 FPs. As shown in Fig. 2, the period of the DT indicated in green is 2. If the sending time of this DT is reserved in each FP, bandwidth resources will be wasted. When it is transmitted from the third to the fourth time slots of every two FPs, bandwidth utilization is increased. In addition, when the DTs are scheduled at the same time slots of every scheduling period, this ensures the periodic transmission of the DTs.

Fig. 3 shows the unfolded CP. When the scheduling of all DTs has been completed, the remaining time slots are used to schedule the BTs. If the sending time of all DTs is reserved in each FP, the scheduling of DTs requires 13 time slots per FP. However, the time slot occupation of DTs can be reduced by a reasonable allocation of bandwidth resources. The scheduling problem of the DT can be converted into a calculation of the minimum time slot occupancy of DTs under the condition that the periodic transmission of the DTs and the sending/receiving link of the NC are not in conflict in any time slot, as follows:

$$\begin{cases} \min \ max\{Task_i.FS + Task_i.length\} \\ s.t. \ Task_i.OTS \cap Task_j.OTS = \emptyset, \quad \forall Task_i, Task_j \in T \end{cases} \tag{5}$$

The term $Task_i.FS$ indicates the starting time slot of the first scheduling of the i-th DT. Moreover, $Task_i.FS + Task_i.length$ is equal to the ending time slot of the first scheduling. As shown in Fig. 2, when the DTs are transmitted periodically, the starting time slot and the ending time slot are same in every scheduling FP, so we can obtain the minimum time slot occupancy by decreasing the maximum ending time slot of the first scheduling of all DTs. Here, $Task_i.OTS$ represents the set of the total time slots occupied by the i-th DT in a CP. When the intersection of any two sets is empty, this indicates that there is no conflict in the transmission of all DTs.

We define $Task_i.OTS_m$ as the set of time slots occupied by the m-th scheduling of the i-th DT in a CP. Since the DTs are periodic, for the starting time slot $Task_i.FS$ of the first scheduling, the starting time slot of the next scheduling is $Task_i.FS + Task_i.length$. In CP, $Task_i.OTS_m$ is given by

$$\begin{aligned} &Task_i.OTS_m \\ &\quad = \{(m-1) * Task_i.period + Task_i.FS, \\ &\qquad (m-1) * Task_i.period + Task_i.FS + 1, \cdots, \\ &\qquad (m-1) * Task_i.period + Task_i.FS + Task_i.length\} \\ &\qquad\qquad \forall m \in \left\{1, 2, \cdots, \frac{CP}{Task_i.period}\right\}, . \end{aligned} \tag{6}$$

Therefore, the $Task_i.OTS$ is the union of all $Task_i.OTS_m$.

$$Task_i.OST = \cup Task_i.OST_m \tag{7}$$

The packing algorithm [25], [26] can make efficient use of resources under the requirement that the boxes do not overlap. These characteristics are in line with the principle that the DT requires efficient scheduling with no conflict. By considering the data of the DTs as "objects" and the bandwidth resources of links as "boxes," the packing algorithm can be applied to the scheduling of DTs.

The packing algorithm is based on best-fit schedules of DTs in a certain order and guarantees that each scheduling is the current optimal solution. In isolation, the optimal solution for bandwidth allocation of DTs can be derived; however, the computational complexity is particularly high, and in fact, it is not necessarily optimal. This is because many of the small-free time slots are difficult to utilize. Therefore, we propose the SS-FP algorithm to simplify the implementation and obtain a more approximate solution for the optimal scheme. The pseudocode of the SS-FP is presented in Algorithm 1.

**Algorithm 1** SS-FP

**Input**: DT set $\boldsymbol{T}$ and link bandwidth time slot matrix $\boldsymbol{B}$
**Output**: Link bandwidth time slot matrix $\boldsymbol{B}$

Initialize $\boldsymbol{B}$;
Calculate the **LCM** and **GCM** of the period and length of DTs
Sort $\boldsymbol{T}$ in ascending order of the period and length of DTs;
**for** $i = 1$ *to* $n$ **do**
  $f_i = Task_i.period/GCM$;
  $FS_i = \{f_{i1}, f_{i2}, \ldots, f_{ij}\}, f_{i1}, f_{i2}, \ldots, f_{ij} \neq 1, f_i$;
  Calculate $STS_{f_i}$ by $STS_{f_i} = ETS_{f_{i-1}} + 1$;
  **for** $p = f_{i1}$ *to* $f_{ij}$ **do**
   **for** $q = FP_1$ *to* $FP_s$ **do**
    **if** $OTS_{pq} + Task_i.length \leq ETS_p$ **then**
     Store $p, q$ in $D = \{(p_1, q_1), (p_2, q_2), \ldots, (p_n, q_n)\}$;
   **end if**
  **end for**
**end for**
Update $\boldsymbol{B}$ and $Task_i.FS$ by minimizing $ETS_p - OTS_{pq} - Task_i.length$;
**if** $D = \varnothing$ **then**
 **for** $q = FP_1$ *to* $FP_s$ **do**
  Update $\boldsymbol{B}$ and $Task_i.FS$ by minimizing $OTS_{f_iq}$;
 **end for**
**end if**
Update $ETS_{f_i} = \max(OTS_{f_iq})$;
**end for**

The FP is the GCD of all DTs; therefore, the period of each DT is an integer multiple of the FP, as follows:

$$Task_i.period = f_i * GCM, \quad f_i \in N_+. \tag{8}$$

Because $f_i$ is a positive integer, $f_i$ can be factorized, and the factor set (FS) of all non-1 and non-f factors of $f_i$ is defined as follows:

$$FS_i = \{f_{i1}, f_{i2}, \ldots, f_{ij}\}, \quad f_{i1}, f_{i2}, \ldots, f_{ij} \neq 1, f_i. \tag{9}$$

If we could centrally schedule DTs with the same cycle, the computational complexity would be significantly reduced. In addition, when we schedule DTs in the order of flow from small to large, low-speed DTs can be used to preferentially fill small-free time slots to increase the time slot utilization. Therefore, we sort all DTs in increasing order of period, and the DTs whose periods are the same are sorted in increasing order of flow. For example, we sorted the DTs in Table 2 in this order.

We define the aggregated time slots (ATS) as the area in which DTs with the same period are scheduled centrally.

**TABLE 2. Task sorting.**

| Number of tasks | Period/GCM | Number of time slots |
|---|---|---|
| 1 | 1 | 2 |
| 2 | 2 | 3 |
| 3 | 2 | 3 |
| 4 | 2 | 3 |
| 5 | 3 | 1 |
| 6 | 3 | 4 |
| 7 | 3 | 6 |
| 8 | 3 | 6 |
| 9 | 4 | 3 |
| 10 | 4 | 3 |
| 11 | 4 | 4 |
| 12 | 4 | 4 |
| 13 | 4 | 4 |
| 14 | 4 | 6 |
| 15 | 6 | 1 |
| 16 | 6 | 3 |
| 17 | 6 | 3 |
| 18 | 6 | 3 |
| 19 | 6 | 4 |
| 20 | 6 | 4 |
| 21 | 6 | 4 |
| 22 | 12 | 1 |
| 23 | 12 | 1 |
| 24 | 12 | 2 |
| 25 | 12 | 2 |
| 26 | 12 | 2 |
| 27 | 12 | 4 |
| 28 | 12 | 4 |

As shown in Fig. 4, we scheduled the DTs with periods 1, 2, 3, 4, 6, and 12. We define the start time slot ($STS_{f_i}$) and end time slot ($ETS_{f_i}$) of the $ATS_{f_i}$ of DTs with period $f_i$. When we have finished scheduling all DTs with period $f_i$, we can obtain the $STS_{f_i}$ and $ETS_{f_i}$ of $ATS_{f_i}$. As shown in Fig. 4 (b), we found that scheduling all DTs with period 2 yields $STS_2 = 3$ and $ETS_2 = 8$.

We define the occupied time slot ($OST_{f_ij}$) as the maximum value of the occupied time slot of the $ATS_{f_i}$ in the j-th FP. As shown in Fig. 4 (c), when all the DTs with period 3 have been scheduled, $OST_{22} = 5$ and $OST_{32} = 12$. Because $ETS_2 = 8$ and $ETS_3 = 15$, there are three free time slots in the second FP of $ATS_2$ and three free time slots in the second FP of $ATS_3$. We have

$$\forall j, \quad STS_{f_i} \leq OST_{f_ij} \leq ETS_{f_i}. \tag{10}$$

After the DTs have been sorted, we need to use the efficient principle to schedule them. The scheduling principle based on the best fit may result in many small-free time slots that cannot be utilized. The implications from Fig. 4(d) provide an instance of it. As shown in it, we found that after we are finished scheduling all the DTs with period 4, if DT 15 is scheduled at the 13th time slot of the 2nd and 8th FP, it will either render the 14th and 15th time slots of the 2nd and 8th FP unutilized or cause a conflict in bandwidth resource allocation. As shown in Fig. 4(e), if DT 15 is scheduled at the 15th time slot of the 3rd and 9th FPs, more consecutive timeslots can be reserved. Therefore, we optimized the scheduling principle based on the best fit. When we need

 

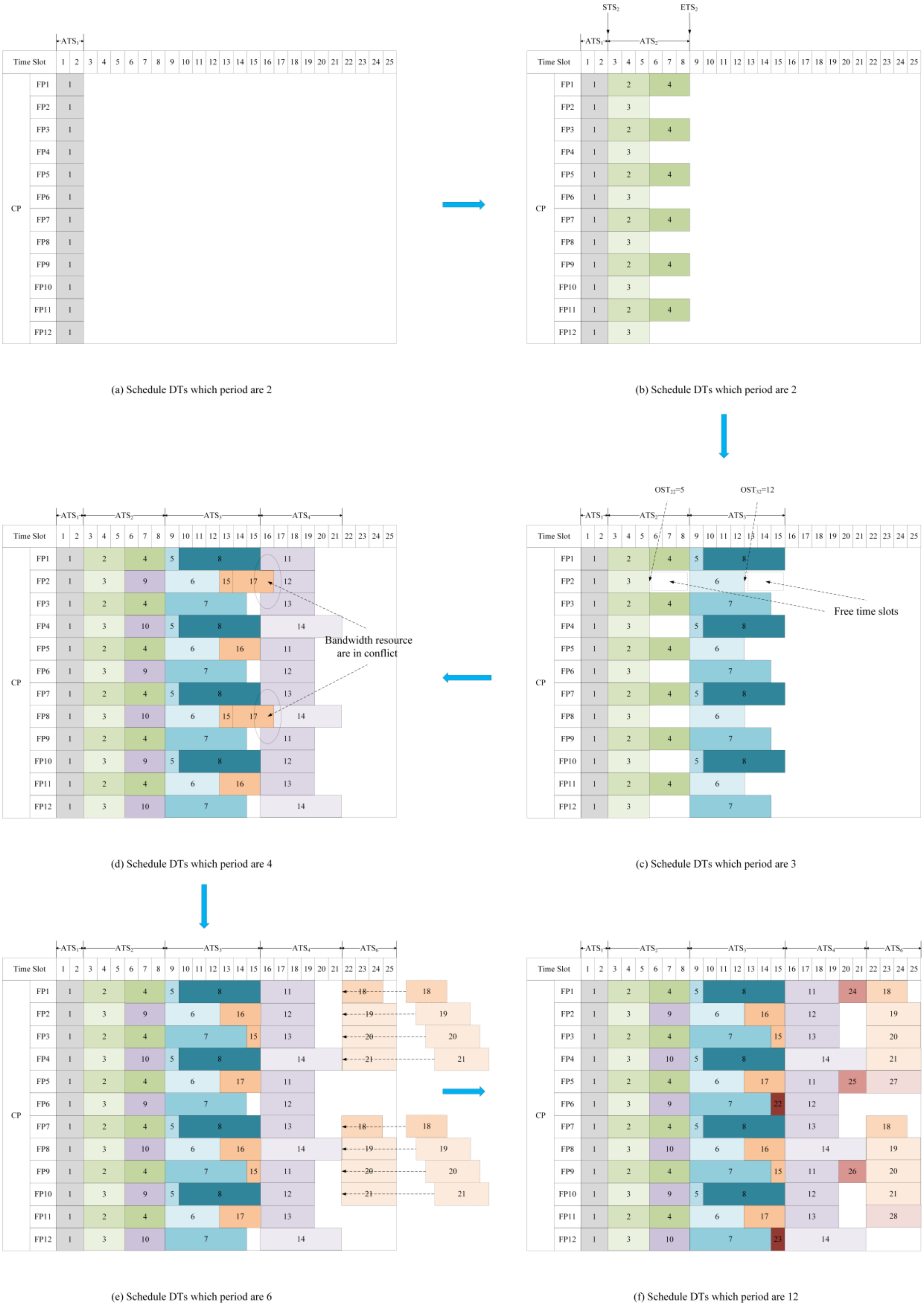


(a) Schedule DTs which period are 2

(b) Schedule DTs which period are 2

(d) Schedule DTs which period are 4

(c) Schedule DTs which period are 3

(e) Schedule DTs which period are 6

(f) Schedule DTs which period are 12

**FIGURE 4.** SS-FP scheduling process.

to schedule a DT, the period is $f_i$. First, we determine each element in the FS of $f_i$. Taking $f_{i1}$ as an example, we determine whether it can be scheduled at the remaining time slots of $ATS_{f_{i1}}$. If it is possible, we schedule the DT at the optimal time slots of $ATS_{f_{i1}}$. When the difference between the number of time slots required by the DT and the remaining time slots of $ATS$ is the smallest, we regard this as the best scheduling option. As shown in Fig. 4(e), the length of DT 15 is 1, and the remaining time slots of the 15th time slot of the 3rd and 9th FPs of $ATS_3$ are also 1. The difference between the two is zero, so this is the optimal time slot to schedule for DT 15. If not, then the other elements of FS are evaluated like $f_{i1}$. As shown in Fig. 4(e), the period of DT 16 is 6; therefore, $FS_{16} = \{2, 3\}$. Since there is no remaining time slot in $ATS_2$, we determine whether there is a remaining time slot in $ATS_3$ or not. DT 16 can be scheduled from the 13th to 14th time slots of the 2nd and 8th FPs. When the DT cannot be scheduled for another ATS, we must determine the FP with the least OST in its own $ATS_{f_{i1}}$. As shown in Fig. 4(e), the DTs 18, 19, 20, and 21 are scheduled in the FP with the least $OST_{f_{ij}}$.

We assume that the CP consists of n FPs and each FP consists of m time slots. As shown in Fig. 3, n=12 and m=25. The time complexity of Algorithm 1 is O($nm$). Because a DT transfers only between the NC and NT, it is only necessary to ensure that the NC sending and receiving link bandwidth resources are allocated without conflict. Because the link is a full-duplex link, the transmission and reception of the DT do not conflict. Considering the worst case, a DT needs to check whether all of the m time slots of $n$ periods are free, and hence the time complexity is O($nm$).

Suppose that the number of full-duplex links is $z$. The spatial complexity of Algorithm 1 is O($nmz$), which is needed to store the link-bandwidth time slot matrix.

In each CP, the NC perceives whether the DTs have changed. If they have, the bandwidth allocation results need to be recalculated; otherwise, the scheduling continues according to the previous scheme. Thus, the SS-FP can adapt to the dynamic changes in DTs. To ensure the periodic transmission of DTs, we schedule DTs with the same period in the specialized ATS. Finally, to improve the transmission efficiency of BTs and to reduce the computational complexity, we schedule low-speed DTs in small-free time slots. Using the above scheme, it is possible to adapt to the changes in DTs and increase the time slot utilization.

### C. DBA-FC

In an FC-AE-1553 network, the size of the BTs is the largest, and this size will increase dramatically in future. The DBA-F schedules BTs in decreasing order of flow to maximize time slot utilization, and the DBA-C schedules BTs in decreasing order of credit ranking to improve fairness. However, both the time slot utilization and fairness should be considered simultaneously. In our scheme, we use delay to characterize the fairness of the network and throughput to characterize time slot utilization. Hence the scheduling problem of BTs can be converted into a problem of calculating the maximum throughput and minimizing the delay under the condition that no links are in conflict in any time slot.

We define the credit ranking matrix C as follows:

$$C = \left[c_{ij}\right]_{n*n} = \begin{bmatrix} c_{11} & \cdots & c_{1(n-1)} & c_{1n} \\ \vdots & & \vdots & \vdots \\ c_{n0} & \cdots & c_{n(n-1)} & c_{nn} \end{bmatrix}. \quad (11)$$

Here, $c_{ij} = \{c|0 \leq c \leq 1\}$. We define $\Delta Task_i.length$ as the difference between the actual allocated bandwidth length and requested bandwidth length from the source address to the destination address of $Task_i$. When $c_{ij} = 0$, the requested bandwidth is equal to the actual allocated bandwidth. When $c_{ij} \neq 0$, the ratio of $\Delta Task_i.length$ and the requested bandwidth $Task_i.length$ is as follows:

$$c_{Task_i source\ Task_i.destination} = \frac{\Delta Task_i.length}{Task_i.length}. \quad (12)$$

As shown in Fig. 5, BT scheduling is a sequential process, and each scheduling result is affected by the previous scheduling result. Therefore, we must update the credit ranking matrix C according to the last scheduling result. To ensure fairness in the network, a higher credit ranking of a BT gives it a higher priority at the next scheduling. Simultaneously, if we can reduce the number of small-free time slots when scheduling BTs, then we can improve the time slot utilization of the network. Because high-speed BTs can occupy bandwidth resources for a long time without wasting them, priority scheduling of high-speed BTs can improve time slot utilization. Hence, BTs with high credit rankings and large lengths should be scheduled preferentially.

When the credit rankings of all the BTs are similar, this indicates that the network is fair. If we prioritize BTs with high credit rankings and ignore the length of the tasks, the time slot utilization will be significantly reduced. Therefore, we should schedule BTs preferentially according to length in this case. Similarly, when the difference in the lengths of all BTs is small, BTs should be scheduled preferentially according to the credit ranking. However, in the situation when some of the BTs have high credit ranking but a smaller length, and the others have low credit ranking but a larger length; then it is difficult to determine the scheduling order.

Because an attention mechanism can focus on important things while ignoring others, we use an attention mechanism based on clustering to solve this problem. First, we define $W_T$ as the weight of the bandwidth request $Task_i.length$ and $W_C$ represents the weight of the credit ranking $c_{ij}$. Two factors should be considered to simultaneously increase the throughput and decrease the delay at the same time. We define the weighted credit ranking $w_i$ of $Task_i$ as in (13), shown at the bottom of the next page.

Next, we cluster the BTs according to their length and credit rating to obtain the degree of difference in the length and credit ranking between BTs. When the difference in the length of all the BTs is small, along with large $W_T$; there will be little distinction among the BTs. This is also

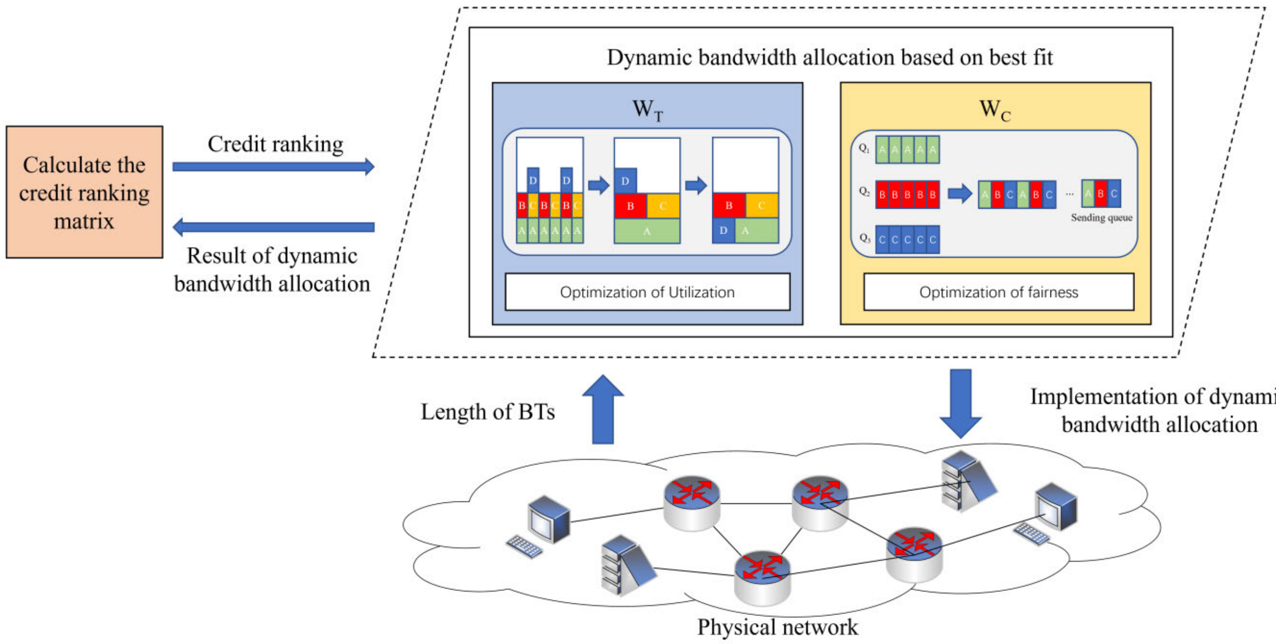


**FIGURE 5.** DBA-FC flow.

true for $W_C$. Therefore, $W_T$ and $W_C$ should be proportional to the distinction in the length of BTs and credit ranking, respectively. Finally, we schedule the BTs in decreasing order of weighted credit ranking $w_i$ based on the best fit. A BT is quite different from a DT. Firstly, because BT is not periodic and secondly, its scheduling sequence has been determined; when we schedule BTs based on the best fit, this will not waste time slots.

Because the length and address of the BTs are variables, $W_T$ and $W_C$ need to be updated online to adapt to the dynamic changes. To obtain the degree of difference in the length of BTs, we divide BTs into high-speed and low-speed task clusters according to the length of the BTs. Then, the mean value of each cluster is calculated and is used as the CC. Finally, the difference between the two mean values indicates the distinction in length. Similarly, we divide BTs into high-credit-ranking and low-credit-ranking task clusters according to the credit ranking matrix C and take the difference between the two mean values as the distinction in credit ranking. The different dimensions of $W_T$ and $W_C$ will affect the final result of $w_i$, and we need to normalize the data to eliminate the influence of the dimensions of the parameters.

We take the length and credit ranking of all BTs as samples and then use the K-means++ algorithm to divide the samples into two clusters as follows:

$$d = \sqrt{\sum_{i=1}^{n} (x_i - y_i)^2} \tag{14}$$

We adopted the Euclidean distance as the distance between the samples. First, a sample is randomly selected as the initialized cluster center (CC). Second, we calculate the Euclidean distance from each sample to the initialized CC, and the sample with the greatest distance is selected as the second CC. Next, the distance from each sample to the two CCs is calculated, and the samples are divided into clusters corresponding to the CCs with the closest distance. Then, the mean value of each cluster is calculated, and the mean value is used to update the CCs. Finally, the last step is repeated, and when the data converge, the optimal CC is obtained.

We define the difference between the two CCs as $\Delta CC$ as follows:

$$\Delta CC = |CC_1 - CC_2|. \tag{15}$$

A larger value of $\Delta CC$ indicates a larger difference between the data sizes of the two clusters. For a normalized representation, we define the maximum value of $\Delta CC$ as $\Delta MCC$ as follows:

$$\Delta MCC = \max\{\Delta CC_1, \Delta CC_2, \cdots \Delta CC_n\}, \tag{16}$$

$$w_i = \frac{1}{2} * \Big(\frac{c_{Task_i.source\ Task_i.destination} - \min(c_{Task_i.source\ Task_i.destination})}{\max(c_{Task_i.source\ Task_i.destination}) - \min(c_{Task_i.source\ Task_i.destination})} * W_C + \frac{Task_i.length - \min(Task_i.length)}{\max(Task_i.length) - \min(Task_i.length)} * W_T\Big) \tag{13}$$

and the NC updates $\Delta MCC$ every FP. Finally, the calculation of the weight is

$$W = \frac{\Delta CC}{\Delta MCC}. \quad (17)$$

The specific process of DBA-FC is as follows. After the bandwidth resource allocation of the DTs is completed, the NC broadcasts and collects the requests of the BTs in each switching domain and updates the task set $T$. We then determine $W_T$ and $W_C$ using the K-means++ algorithm. Because the initial credit rankings are all zero, $W_T = 1$ and $W_C = 0$ at the first scheduling. Then, for each subsequent scheduling, the weighted credit ranking should be calculated according to (13). Next, we sort the BTs according to the value of the weighted credit ranking in descending order and then allocate the bandwidth by the principle based on the best fit. Simultaneously, we update the link bandwidth time slot matrix $B$ and the credit ranking matrix $C$. The pseudocode of this algorithm is presented in Algorithm 2.

**Algorithm 2** DBA-FC

**Input**: BT set $\boldsymbol{T}$, link bandwidth time slot matrix $\boldsymbol{B}$, and credit ranking matrix $\boldsymbol{C}$

**Output**: Link bandwidth time slot matrix $\boldsymbol{B}$, credit ranking matrix $\boldsymbol{C}$, the weight of credit ranking $\boldsymbol{W}_C$, and the weight of task length $\boldsymbol{W}_T$

01. Divide BTs into a high-speed task cluster and low-speed task cluster by the K-means++ algorithm;
02. Update $\Delta MCC$ by $\Delta MCC = \max\{\Delta CC_1, \Delta CC_2, \cdots \Delta CC_n\}$;
03. Update $\boldsymbol{W}_T$ by $W = \Delta CC/\Delta MCC$;
04. Divide BTs into a high-credit ranking task cluster and low- credit ranking task cluster by the K-means++ algorithm;
05. Update $\Delta MCC$ by $\Delta MCC = \max\{\Delta CC_1, \Delta CC_2, \cdots \Delta CC_n\}$;
06. Update $\boldsymbol{W}_C$ by $W = \Delta CC/\Delta MCC$;
07. **for** $i = 1$ *to* $n$ **do**
08. Calculate $w_i$ by $w_i = \frac{1}{2} * (\frac{c_{Task_i.source\ Task_i.destination} - \min(c_{Task_i.source\ Task_i.destination})}{\max(c_{Task_i.source\ Task_i.destination}) - \min(c_{Task_i.source\ Task_i.destination})} * W_C + \frac{Task_i.length - \min(Task_i.length)}{\max(Task_i.length) - \min(Task_i.length)} * W_T)$
09. **end for**
10. Sort $\boldsymbol{T}$ in decreasing order of $w_i$;
11. **for** $i = 1$ *to* $n$ **do**
12. Update $\boldsymbol{B}$ using the packing algorithm based on best fit;
13. Update $\boldsymbol{C}$ by $c_{Task_i.source\ Task_i.destiantion} = \frac{\Delta Task_i.length}{Task_i.length}$;
14. **end for**

Suppose there are $x$ switching domains in the network, each switching domain has $y$ nodes, and the number of full-duplex links is $z$. Each node must connect to the switch of its own switching domain, which requires $xy$ links. Even when the star topology or serial topology is adopted, at least $x-1$ links are required. Thus, to ensure that any two switching domains are interconnected, we must have that $z > xy+x-1$. The BT transmission period of one FP is divided into $K$ time slots, and each time slot can transmit at least one complete data frame.

When BTs are transmitted in the same switching domain, only the sending link of the source address and the receiving link of the destination address of the BTs need to be checked; therefore, the average time complexity of Algorithm 2 is $O(x(y^2-y)K)$. When BTs are transmitted in different switching domains, it is also necessary to consider the link bandwidth resources between the switching domains. There are $z - xy$ links between switching domains and therefore, the average time complexity of Algorithm 2 is $O((z - xy)K + (x^2 - x)y^2K)$.

The space complexity of Algorithm 2 is $O(x^2y^2 + zk)$, which is used to store the BT bandwidth request matrix T and link bandwidth time slot matrix B.

When we schedule the BTs, we consider both fairness and time slot utilization simultaneously. The length and credit ranking of the BTs are weighted, and the BTs are then scheduled in descending order of the sum of the two weights. To adapt to the dynamic changes in BTs, $W_T$ and $W_C$ need to be updated online according to the difference in the length and credit ranking of the BTs. We use the K-means++ algorithm to cluster the BTs according to their sizes and then determine the value of $W_T$ and $W_C$. Using the above scheme, it is possible to trade-off the throughput and the delay of the network.

### D. OVERVIEW OF MTHSS

Fig. 6 shows the multitask scheduling of a CP, where a CP consists of n FPs. Each FP is divided into three parts: the DT scheduling period, the collection and calculation period, and the BT scheduling period. As shown in Fig. 7, the experimental network has a total of 27 full-duplex links; the links numbered $1, 2, \ldots, 27$ are the sending links, and the links numbered $28, 29, \ldots, 54$ are the receiving links. We divide the bandwidth resources of each link into several time slots, where each block represents a time slot of the link. The red blocks represent the transmission of the ITs. The ITs can only be randomly generated by the NC and must be transmitted immediately.

Before the first scheduling, the NC determines the CP and FP according to the periods of the DTs in the entire network, and then it schedules the DT in a CP according to the SS-FP. Each subsequent scheduling of the DT is executed based on the results of this calculation. However, if the length and number of DTs change, the NC updates the scheduling scheme in the subsequent CP.

After DT transmission is completed, the NC broadcasts the command frames separately in each switching domain and then collects the report frames from the NTs. The NC allocates bandwidth resources using the DBA-FC to improve the concurrency of transmission.

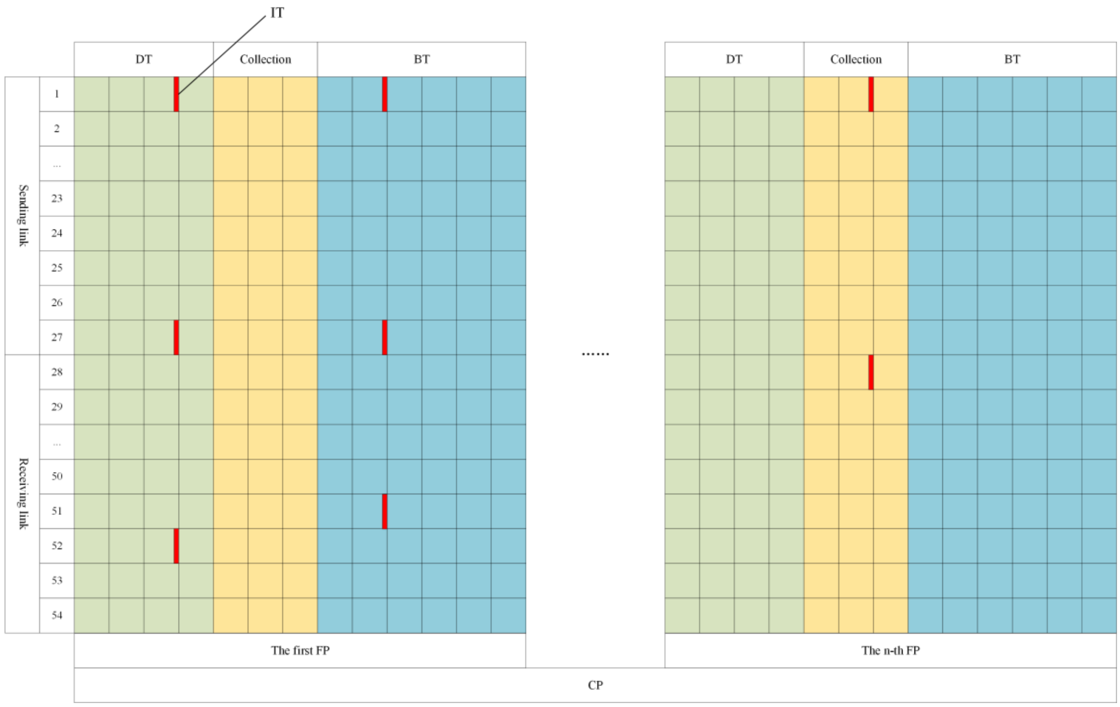


**FIGURE 6.** Dynamic and static hybrid scheduling schemes based on slot allocation.

For ITs, there is no fixed time slot for their transmission. The length of the ITs is very small, so we reserve the sending times of ITs in the bandwidth allocation of the DTs and BTs to ensure timeliness of ITs. An IT uses preemptive bandwidth allocation, i.e., it checks whether there is an IT to be sent in every time slot. Once an IT has been generated, it must be transmitted immediately. As shown in Fig. 6, an IT can be transmitted at any period of each scheduling period and is only generated by the NC. After it has been generated, it occupies the bandwidth resources of the sending link of the NC and the transmission resources of the other related links.

The MTHSS is a centralized scheduling mechanism based on time slot allocation. The MNC centrally controls the transmission of all data and makes quick and consistent decisions for end-to-end transmission. In addition, owing to the periodicity of the DTs, we divided the aggregated time slots according to the period to improve the time slot utilization of DTs. For the scheduling of the BTs, we improve the fairness and time slot utilization of the network according to credit value and length. We preemptively schedule the ITs to ensure timeliness.

## IV. EXPERIMENTS AND EVALUATION

We conducted a performance analysis of our hybrid scheduling scheme by establishing the appropriate experimental scenarios. The tests included the performance of SS-FP, the performance of DBA-FC, and their comprehensive performance in the FC-AE-1553 multi-level switching network.

### A. EXPERIMENTAL SCENARIO

In the simulation, we used the topology shown in Fig. 7. It contains one NC, 23 NTs, three switches, and 27 full-duplex fiber links, with a transmission rate of 10 Gbps. For convenience and brevity, we numbered the devices in the network and in the links. The parameters in parentheses represent the IDs of devices and links. Because the links are full duplex, each physical link has two IDs.

A random communication task was designed to examine the impact of the algorithm on network evaluation metrics such as the bandwidth resource utilization, data transmission delay, and throughput. Source node $i$ was randomly selected and another node $j$ was randomly selected as the destination. For the DTs and ITs, either the source or the destination address must be the NC; but for the BTs there was no such restriction. The period of the DTs was a randomly selected value from 1–10 ms in intervals of 1 ms, but the generation times of BTs and ITs were random. Table 1 lists the details of the tasks used in our experiments, and we assume that the minimum length of a data frame is 100 bytes. Because the frames are transmitted according to the 8 b/10 b ratio encoding, the length of the DTs, BTs and ITs is 1000–5120 bits, 1–640 Kbits, and 1000 bits, respectively. The link for each task is the shortest path calculated according to the topology shown in Fig. 7 and so we used the static routes to transmit the data.

### B. PERFORMANCE OF THE SS-FP

To test whether the SS-FP can adapt to dynamic changes in DTs, we used a random communication task to simulate the

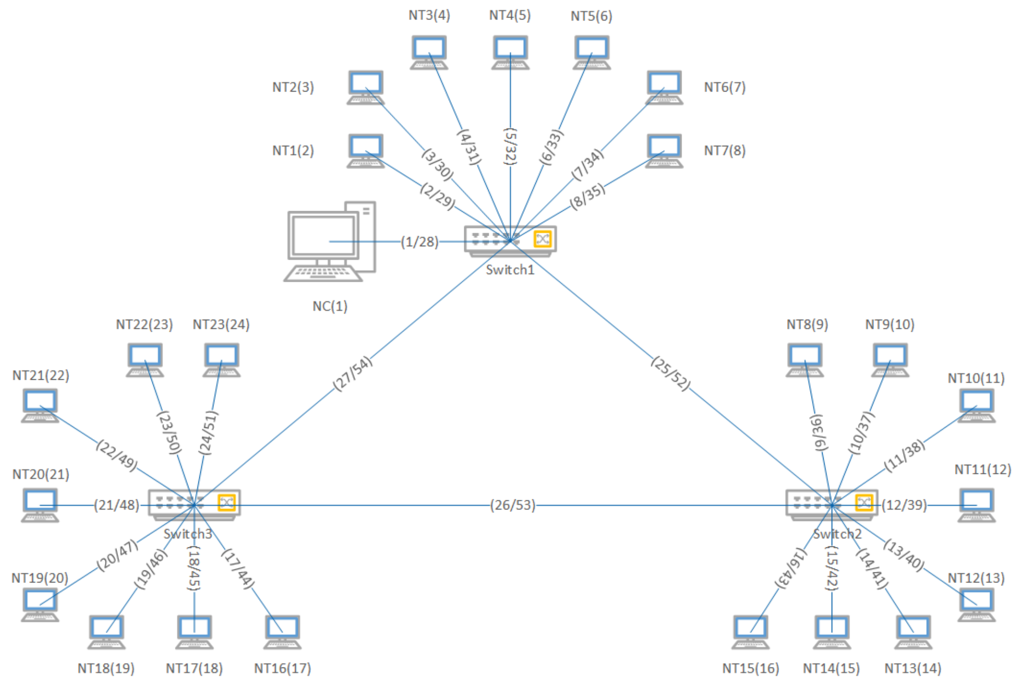


**FIGURE 7.** Experimental network topology.

**TABLE 3.** Time slot occupancy results of the DTs.

| Method | Number of DTs | | | | | | | | | |
|---|---|---|---|---|---|---|---|---|---|---|
| | 10 | 20 | 30 | 40 | 50 | 60 | 70 | 80 | 90 | 100 |
| Original | 0.0411 | 0.0813 | 0.1211 | 0.1606 | 0.2004 | 0.2405 | 0.2808 | 0.3205 | 0.3610 | 0.4005 |
| Packing | 0.0276 | 0.0477 | 0.0540 | 0.0617 | 0.0671 | 0.0729 | 0.0804 | 0.0893 | 0.0992 | 0.1076 |
| SS-FP | 0.0221 | 0.0340 | 0.0432 | 0.0502 | 0.0576 | 0.0646 | 0.0727 | 0.0797 | 0.0883 | 0.0962 |

**TABLE 4.** Time slot utilization results of the DTs.

| Method | Number of DTs | | | | | | | | | |
|---|---|---|---|---|---|---|---|---|---|---|
| | 10 | 20 | 30 | 40 | 50 | 60 | 70 | 80 | 90 | 100 |
| Original | 0.1906 | 0.1962 | 0.1975 | 0.1956 | 0.1965 | 0.1959 | 0.1981 | 0.1963 | 0.1980 | 0.1988 |
| Packing | 0.2831 | 0.3343 | 0.4428 | 0.5091 | 0.5863 | 0.6455 | 0.6915 | 0.7044 | 0.7203 | 0.7395 |
| SS-FP | 0.3602 | 0.4712 | 0.5542 | 0.6247 | 0.6828 | 0.7285 | 0.7645 | 0.7884 | 0.8087 | 0.8274 |

number and lengths of different tasks in the network. When the number of tasks is sufficiently large, it is not difficult to calculate the CP as 2520 ms and a FP of 1 ms. Each FP was divided into 1000 time slots, which means that the length of one time slot was 1 $\mu$s. We assumed that the length and number of DTs would change in every CP and therefore, repeated 500 experiments to eliminate random errors.

We tested the performance of our proposed static scheduling scheme and compared it with the performance of a packing algorithm based on the best fit and the performance of the most primitive scheduling scheme. The experimental results are shown in Tables 3 and 4 after taking the average value, and the results of the random experiments are plotted in Figs. 8 and 9.

The time slot occupancy of the DTs indicates the proportion of time slots occupied by the DTs with respect to the time slots of the entire FP. When the total time slots of an FP remain unchanged, the small time slot occupancy of the DTs increases the transmission time slots and improves the transmission quality of the BTs. As Fig. 8 shows, the time slot occupancy of the three schemes is proportional to the number of tasks. When the number of tasks is doubled, the time slot occupancy of the original scheme, packing algorithm based on the best fit, and the SS-FP increases by

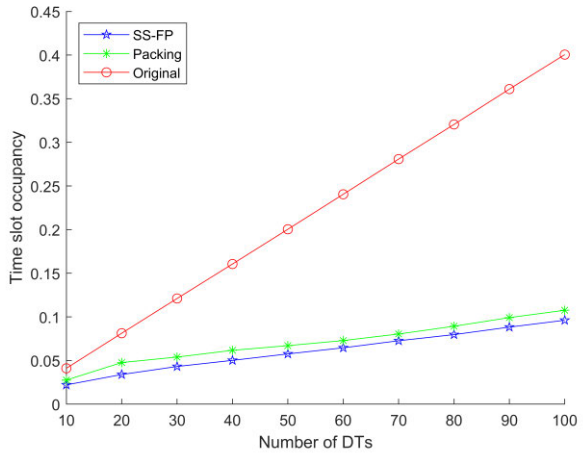


**FIGURE 8.** Time slot occupancy of the DTs.

0.9983, 0.2741, and 0.2058, respectively. When the bandwidth resources are reserved for each FP using the original scheme, a large amount of bandwidth resources are wasted, which leads to a rapid increase in the time slot occupancy. While the packing algorithm improves the concurrency of transmission while avoiding link conflicts, the number of small-free time slots that are difficult to utilize will increase the time slot occupancy. The SS-FP takes advantage of the periodicity of the DTs to reduce their time slot occupancy. The experimental results show that the SS-FP can reserve more bandwidth resources and can provide a higher quality of service for BTs.

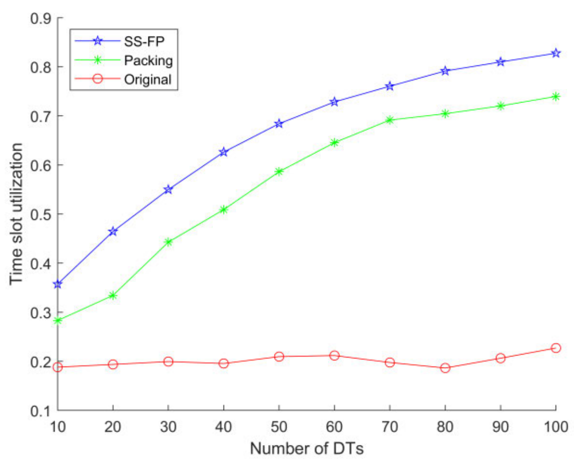


**FIGURE 9.** Time slot utilization rate of the DTs.

When analyzing the performance of different schemes in this study, we focus only on time slot utilization. We ignore the transmission delay in the link, processing and forwarding delay in the switch, and sending delay of each terminal. This is because these delays only affect the sending and receiving times of the scheduling table and not the time slot utilization of the link. The time slot utilization of the DTs indicates the proportion of the time slots used to transmit the DTs to the time slots occupied by the DTs. As can be seen from Fig. 9, because the original scheme does not consider data concurrency, the utilization of the original scheme is approximately 19.65% which does not change with an increase in the number of tasks. When the number of DTs is greater than 100, the utilization of link resources can no longer be significantly improved. At this time, the utilization of the SS-FP is 10% higher than that of the packing algorithm. Because the SS-FP takes advantage of the periodicity of the DTs while considering data concurrency, it can improve the time slot utilization better than the packing algorithm. To be specific, we aggregate the time slots, and the DTs with the same period can be scheduled together to reduce the number of small-free time slots and to improve time slot utilization. Then, we sort the DTs in a certain order, and the low-speed tasks are prioritized. We determine whether a DT can be scheduled in a small-free time slot. If not, then we schedule the DT in the ATS, which further improves the time slot utilization.

### C. PERFORMANCE OF DBA-FC

When analyzing the performance of DBA-FC, we assume that the state of the network is ideal, i.e., there is no network congestion or packet loss during transmission. In the experiment, the transmission rate of the link was defined as 10 Gbps, the FP was 1 ms and the system was divided into 1000 time slots. We used a random communication task to simulate the flows of the network and then, we tested the performance of the DBA-FC and compared it with the DBA-F and DBA-C schemes. We analyzed the impact of the different schemes on the average delay, maximum delay, and throughput of the network. The results are shown in Table 5.

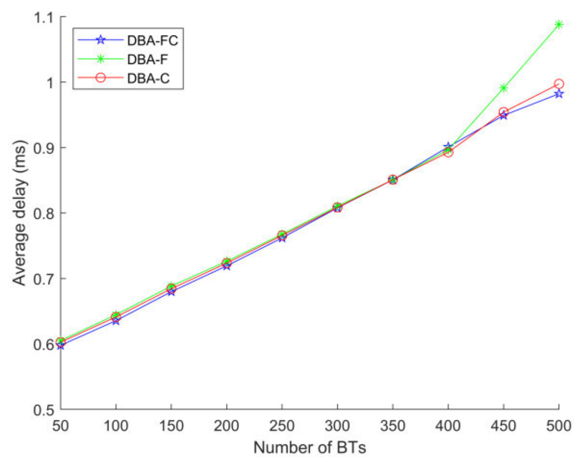


**FIGURE 10.** Impact on average delay.

To evaluate the impact of flows on average delay, flows are gradually added to a network until the packet loss rate becomes non-zero. As shown in Fig. 10, when the number of BTs is less than 350, the average delay is similar for all the three schemes because the bandwidth requests of the

**TABLE 5. Comprehensive performance of the network for various dynamic bandwidth allocation schemes.**

| Number of BTs | Average delay (ms) | | | Maximum delay (ms) | | | Throughput (Gbps) | | |
|---|---|---|---|---|---|---|---|---|---|
| | DBA-C | DBA-F | DBA-FC | DBA-C | DBA-F | DBA-FC | DBA-C | DBA-F | DBA-FC |
| 50 | 0.6027 | 0.6052 | 0.5979 | 1.2508 | 16.2051 | 1.2848 | 16.2051 | 16.2051 | 16.2051 |
| 100 | 0.6412 | 0.6446 | 0.6356 | 1.4428 | 32.3020 | 1.4428 | 32.3020 | 32.3020 | 32.3020 |
| 150 | 0.6844 | 0.6884 | 0.6799 | 1.5399 | 48.3771 | 1.5399 | 48.3771 | 48.3771 | 48.3771 |
| 200 | 0.7235 | 0.7264 | 0.7193 | 1.6998 | 64.4091 | 1.6706 | 64.4091 | 64.4091 | 64.4091 |
| 250 | 0.7657 | 0.7677 | 0.7620 | 1.7547 | 80.8007 | 1.7914 | 80.8007 | 80.8007 | 80.8007 |
| 300 | 0.8085 | 0.8106 | 0.8080 | 3.5801 | 96.8628 | 2.2568 | 96.8628 | 97.0373 | 97.0373 |
| 350 | 0.8510 | 0.8508 | 0.8508 | 4.6478 | 111.3786 | 4.4368 | 111.3786 | 113.3192 | 113.3192 |
| 400 | 0.8928 | 0.8968 | 0.9010 | 25.3603 | 118.8435 | 9.0614 | 118.8435 | 128.8749 | 129.5847 |
| 450 | 0.9542 | 0.9909 | 0.9492 | 40.7203 | 120.7656 | 35.6872 | 120.7656 | 140.5541 | 145.7278 |
| 500 | 0.9973 | 1.0880 | 0.9822 | 50.5937 | 122.1872 | 36.5681 | 122.1872 | 145.1144 | 158.9704 |

BTs are all satisfied. When the number of BTs is greater than 350, the average delays of DBA-FC and DBA-C are smaller than that of DBA-F. However, between DBA-FC and DBA-C, a slight difference in the average delay was observed. DBA-C decides the next scheduling result based only on the previous scheduling results, but DBA-FC considers the length of the next BT bandwidth request. Therefore, when the packet loss rate is 0, our solution reduces the average delay by approximately 2%, when compared with DBA-C.

As shown in Figs. 10 and 11, the average and maximum delays increase with the network load. However, the maximum delay of DBA-F is much higher than those of DBA-FC and DBA-C. DBA-F determines the next scheduling result based only on the length of the bandwidth requests of the BTs. When the NC receives all bandwidth requests, the NC schedules them in decreasing order of length, which may lead to the starvation of low-speed tasks. When the number of BTs is less than 350, the maximum delays of DBA-FC and DBA-C are less than 5 ms. When the number of BTs is greater than 350, the maximum delay for DBA-FC is smaller than that for DBA-C. This is because SS-FP considers the length of the DTs, which reduces the queuing delay for high-speed DTs.

The throughput increases with an increase in the network load, and when the maximum throughput of the scheduling mechanism is reached, the throughput becomes saturated. At this time, packet loss occurs in the network. As shown in Fig. 12, the DBA-FC is significantly better than the other two schemes. The maximum throughput results of DBA-FC, DBA-F, DBA-C are 159.0 Gbps, 128.9 Gbps, and 111.4 Gbps, respectively. When the scheduling of BTs considers only the flow; although the priority scheduling of high-speed BTs can improve the utilization of bandwidth resources, it may cause other BTs to be unable to transmit. It happens because the bandwidth resources of the links are occupied all the time, thereby reducing the throughput at a certain level. When the scheduling of the BTs only considers the credit ranking, the algorithm based on the best fit can reduce the number of small-free time slots, but it cannot utilize the bandwidth in an overall efficient manner. In contrast, our scheme can combine the advantages of the above two methods. Hence, it not only

**TABLE 6.** Comprehensive performance of the network.

| Network load | DT (µs) | | BT (ms) | | IT (µs) | | Throughput( Gbps) | Packet loss rate (%) |
|---|---|---|---|---|---|---|---|---|
| | Maximum delay | Average delay | Maximum delay | Average delay | Maximum delay | Average delay | | |
| 0.1 | 25.61 | 20.08 | 1.34 | 0.63 | 30.03 | 5.23 | 27.89 | 0 |
| 0.2 | 24.93 | 20.34 | 1.56 | 0.69 | 29.56 | 5.98 | 54.31 | 0 |
| 0.3 | 24.71 | 19.76 | 1.68 | 0.76 | 29.16 | 6.80 | 82.86 | 0 |
| 0.4 | 25.43 | 19.77 | 3.16 | 0.83 | 29.58 | 9.76 | 111.61 | 0 |
| 0.5 | 25.71 | 19.95 | 13.17 | 0.91 | 30.11 | 11.44 | 139.55 | 0 |
| 0.6 | 24.89 | 20.17 | 36.35 | 1.01 | 30.12 | 14.25 | 167.35 | 0 |

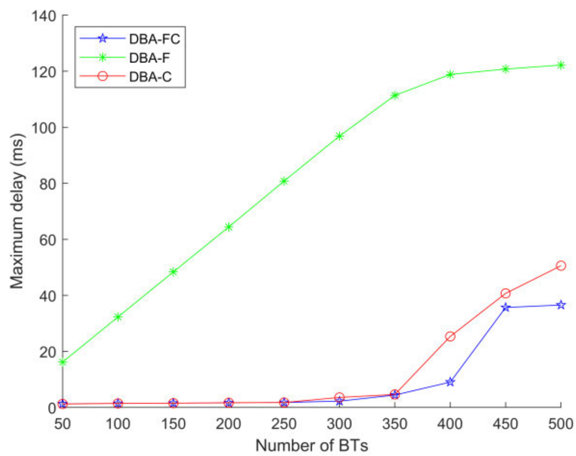


**FIGURE 11.** Impact of DBA scheme on maximum delay.

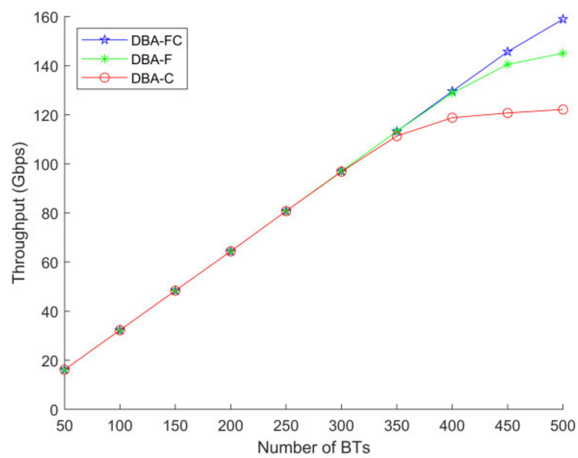


**FIGURE 12.** Impact of DBA scheme on throughput.

utilizes the bandwidth resources as a whole but also reduces the number of small-free time slots and improves the time slot utilization.

### *D. COMPREHENSIVE PERFORMANCE*

To test the comprehensive performance of MTHSS, the ITs were added, and 0.1 $\mu$s sending time was reserved for IT every 30 time slots when allocating the bandwidth.

It follows from Table 6 that our proposed scheme can achieve the expected results, and the maximum transmission delay of each task is less than the maximum allowable delay. The throughput of the FC-AE-1553 multi-level switching network increases with an increase in network load. When the network load is 0.6, the throughput is 167.35 Gbps. The maximum delay of the ITs is approximately 30 $\mu$s. This is because we reserve a sending time for ITs every 30 time slots. Further, the average delay of the ITs increases with an increase in load. As the network load increases, the probability of an IT being generated at the same time as other tasks being transmitted by the NC increases.

## V. CONCLUSION

Recently, there has been an increase in the requirements of avionics communication systems and ship electromechanical communications for throughput, reliability, and real-time operation. In response to it, we proposed the MTHSS for FC-AE-1553 multi-level switching networks under centralized control to make quick and consistent decisions regarding end-to-end transmissions. The SS-FP and DBA-FC were also given. The SS-FP aggregates the time slots according to the period and then allocates the bandwidth in a certain order. The DBA-FC updates the parameters online based on the differences in the lengths and credit ratings of the BTs. The experimental results show that the SS-FP improves the bandwidth utilization by 10% and the DBA-FC balances throughput and delay. Our scheme can not only be applied in an FC-AE-1533 network, but also in a time triggered network. In our future work, we will research methods to further improve the utilization of bandwidth resources and comprehensive performance so that the actual demands of avionics communication and ship electromechanical communications can be met.

## REFERENCES

[1] Z. Gao, G. Huang, and X. Qi, "Research on FC-AE-1553 bus acquisition technology," in *Proc. IEEE Int. Conf. Artif. Intell. Inf. Syst. (ICAIIS)*, Dalian, China, Mar. 2020, pp. 20–22.
[2] L. Fang, G. Zhao, and S. Cao, "Performance evaluation of FC-AE-1553 network transmission," *J. Beijing Univ. Aeronaut. Astronaut.*, vol. 41, no. 8, pp. 1396–1402, Aug. 2015.
[3] X. Cha, J. Nan, and H. Luo, "Design of protocol converting scheme between FC-AE-1553 and MIL-STD-1553," *Comput. Eng. Des.*, vol. 33, no. 3, pp. 895–900, Jun. 2012.
[4] G. Cossu, L. Gilli, E. Ertunc, and E. Ciaramella, "Transporting MIL-STD-1553 signals by means of optical wireless interfaces," *IEEE Photon. J.*, vol. 14, no. 1, pp. 1–8, Feb. 2022.
[5] J. Yao, J. Wu, Q. Liu, Z. Xiong, and G. Zhu, "System-level scheduling of mixed-criticality traffics in avionics networks," *IEEE Access*, vol. 4, pp. 5880–5888, 2016.
[6] Q. Xu and X. Yang, "Performance analysis on transmission estimation for avionics real-time system using optimized network calculus," *Int. J. Aeronaut. Space Sci.*, vol. 20, no. 2, pp. 506–517, Jun. 2019.
[7] G. Dahman, F. Gagnon, and G. Poitau, "Ship-to-ship beyond line-of-sight communications: A comparison between ray tracing simulations and the PETOOL," in *Proc. 32nd Gen. Assem. Sci. Symp. Int. Union Radio Sci. (URSI GASS)*, Aug. 2017, pp. 1–4.
[8] D. Gao, T. Li, Y. Sun, W. Wang, H. Hu, J. Meng, Y. Zheng, and X. Xie, "Latest developments and trends of space laser communication," *Chin. Opt.*, vol. 11, no. 6, pp. 901–913, 2018.
[9] Y. Dong, "Development status of avionics airborne communication technology," *Technol. Innov. Appl.*, vol. 22, no. 12, pp. 133–134, Aug. 2020.
[10] L. Lombardo, S. Corbellini, M. Parvis, A. Elsayed, E. Angelini, and S. Grassini, "Wireless sensor network for distributed environmental monitoring," *IEEE Trans. Instrum. Meas.*, vol. 67, no. 5, pp. 1214–1222, May 2018.
[11] B. Chen and C. Yang, "Energy costs for traffic offloading by cache-enabled D2D communications," in *Proc. IEEE Wireless Commun. Netw. Conf.*, Apr. 2016, pp. 1–6.
[12] X. Yan, J. Li, and B. Mei, "Collaborative optimization design for centralized networked control system," *IEEE Access*, vol. 9, pp. 19479–19487, 2021.
[13] A. Bhatia and R. C. Hansdah, "A distributed TDMA slot scheduling algorithm for spatially correlated contention in WSNs," *Mobile Inf. Syst.*, vol. 2015, pp. 1–16, Jan. 2015.
[14] X. Ge, F. Yang, and Q.-L. Han, "Distributed networked control systems: A brief overview," *Inf. Sci.*, vol. 380, pp. 117–131, Feb. 2017.
[15] J. Wang, "Research on dynamic scheduling mechanism of FC-AE-1553 network services," Beijing University of Posts and Telecommunications, Beijing, China, Tech. Rep., 2017.
[16] H. Qian, W. He, and F. Song, "Research on data node scheduling method for distributed network carrier communication," *Electron. Des. Eng.*, vol. 27, no. 21, pp. 108–112, Nov. 2019.
[17] G. Jiang, L. Sun, H. Zhang, C. Ma, and Z. Zhang, "Study of dynamic bandwidth allocation algorithm based on FC-AE-1553 PON network in air-space electronic network," *Navigat. Control*, vol. 17, no. 1, pp. 34–41, Mar. 2018.
[18] J. Huang, "The characteristics of FC-AE-1553 data bus and its application in aerospace field," *Astron. Syst. Eng. Technol.*, vol. 5, no. 4, pp. 67–72, Jul. 2021.
[19] Y. He, L. Wang, Y. Zhan, S. Cao, and X. Luo, "Dynamic bandwidth scheduling algorithm for space applications in FC-AE-1553 switching network," in *Proc. Asia Commun. Photon. Conf. (ACP)*, Hangzhou, China, Oct. 2018, pp. 1–3.
[20] S. Wu, Y. Zhan, K. Qiao, J. He, X. Chang, and L. Wang, "Scheduling mechanism of FC-AE-1553 network based on credit ranking," in *Proc. 14th Int. Conf. Wireless Mobile Comput., Netw. Commun. (WiMob)*, Limassol, Cyprus, Oct. 2018, pp. 1–8.
[21] M. Liu and L. Zhang, "Resource allocation for D2D underlay communications with proportional fairness using iterative-based approach," *IEEE Access*, vol. 8, pp. 143787–143801, 2020.
[22] J. Li, L. Wang, S. Wu, Y. Zhan, S. Cao, J. Wang, and X. Chen, "A multi-service QoS supported DBA algorithm based on concurrency for FC-AE-1553 PON network," in *Proc. Asia Commun. Photon. Conf.*, Wuhan, China, 2016, pp. 1–3.
[23] Y. Zhan, L. Wang, J. Li, J. Wang, S. Wu, and S. Cao, "Static + dynamic bandwidth allocation for PON FC-AE-1553 network," in *Proc. 15th Int. Conf. Opt. Commun. Netw. (ICOCN)*, Hangzhou, China, Sep. 2016, pp. 1–3.
[24] T. Lan, Z. Dong, H. Zhang, and J. Guo, "An autonomous inter-device bus control transfer protocol for time synchronization 1553B bus network," in *Proc. Int. Conf. Commun., Signal Process., Syst.*, Singapore, Jun. 2021, pp. 354–361.
[25] Y. Guo, "TTE scheduling table generation algorithm based on two-dimensional packing problem," *Comput. Eng. Des.*, vol. 42, no. 8, pp. 2159–2166, Aug. 2021.
[26] T. Yang, F. Luo, W. Ding, and H. Lu, "Bin packing algorithm based on adaptive optimization of slack," *Comput. Sci.*, vol. 47, no. 4, pp. 211–216, Apr. 2020.

**HAO LI** received the B.Eng. degree in electronic information engineering from the Wuhan University of Science and Technology, in 2021. He is currently pursuing the master's degree with Wuhan University. During his B.Eng. studies, he won three university-level scholarships. He will continue to pursue the Ph.D. degree in software-designed networking (SDNs). His research interests include network simulation and the technology of future networks.

**NINGNING LU** graduated from Beijing Jiaotong University, in 2011. He started work as an Engineer at the 54th Research Institute, China Electronics Technology Group Corporation (CETC), in 2012, where he is currently a Senior Engineer. His research interests include the IoT, machine type communication, and routing and switching technology.

**HAO WANG** received the B.S. and Ph.D. degrees from the School of Electronic Information, Wuhan University, China, in 2008 and 2013, respectively. He was a Visiting Scholar with the Department of Electrical and Computer Engineering, University of Calgary, Canada. He is currently a Senior Engineer with the Wuhan Second Ship Design and Research Institute, Wuhan, China. His research interests include ship design, automation, and control system design.

**LIHUA WU** received the B.S. and Ph.D. degrees from the School of Electronic Information, Wuhan University, China, in 2009 and 2016, respectively. He was a Visiting Scholar with the Department of Electrical and Computer Engineering, University of Calgary, Canada. He is currently a Senior Engineer with the No. 5 Laboratory, Wuhan Second Ship Design and Research Institute, Wuhan, China. His research interests include ship information, complex networks, wireless communication networks, and mobile internet.

**JING WU** (Member, IEEE) received the B.Eng. and Ph.D. degrees in communication and information systems from Wuhan University, China, in 2002 and 2007, respectively. From 2009 to 2010, she was a Postdoctoral Researcher at LIMOS, Clermont-Ferrand, France. She is currently an Associate Professor with Wuhan University and a part-time Associate Researcher with the Collaborative Innovation Center of Geospatial Technology. Her research interests include software-defined intelligent networks, distributed network simulation, and satellite/terrestrial integrated networks.

**HAO JIANG** (Member, IEEE) received the B.Eng. degree in communication engineering and the M.Eng. and Ph.D. degrees in communication and information systems from the Electronic Information School, Wuhan University, China, in 1999, 2001, and 2004, respectively. From 2004 to 2005, he was a Postdoctoral Researcher with LIMOS, Clermont-Ferrand, France. He was also a Visiting Professor with the University of Calgary, Canada, and ISIMA, Blaise Pascal University, France. He is currently a Professor with the Electronic Information School, Wuhan University. He has authored more than 60 papers in different journals and conferences. His research interests include artificial intelligence, social computing, and mobile big data.

**JIANGUO ZHOU** was born in 1965. He received the B.Eng. degree in computer and automation from Sichuan University, China, in 1988, and the M.Eng. degree in radio electronics and the Ph.D. degree in communication and information systems from Wuhan University, China, in 1991 and 2013, respectively. He is currently an Associate Professor with Wuhan University. He has authored more than 50 papers in different journals and conferences. His research interests include computer networks and spatial information networks. He serves as a Senior Member for the China Institute of Communications.